Tight-binding molecular dynamics study of mechanical and electronic properties in twisted graphene nanoribbons

Satofumi Souma†, Shozo Kaino, and Matsuto Ogawa
Department of Electrical and Electronic Engineering, Kobe University, Kobe 657-8501, Japan
†email: ssouma@harbor.kobe-u.ac.jp

***Abstract*—We study numerically the effect of mechanical twisting on the geometrical and electronic properties of graphene nanoribbon (GNR) devices. By employing the tight-binding molecular dynamics method for structural relaxation calculations in the presence of twisting, we found that the geometry of the twisted GNR changes abruptly when the twisting angle exceeds a threthold angle. Moreover it has been found that such twisting induced abrupt change in the geometry of AGNR can actually cause the abrupt change in the electronic property as well.**

I. Introduction

Since the experimental success in the exfoliation of single layer graphene (SLG) in 2004 [1], [2], [3], various types of graphene based new functional devices have been proposed, including the bi-layer graphene transistors, graphene nanoribbon transistors, spin filters, gas sensors, pressure sensors, and so on [4], [5], [6], [7]. Among these interesting devices based on graphene, the idea to engineer the electronic properties by introducing the mechanical deformation is especially important since it is one of special features which can be most flexibly designed if we use graphene as base materials. Having motivated by such interesting properties of graphene, here we study another graphene based electromechanical devices, the twisted graphene nanoribbon (GNR) devices, where the electronic properties of GNR are expected to be modulated by changing the twisting angle.

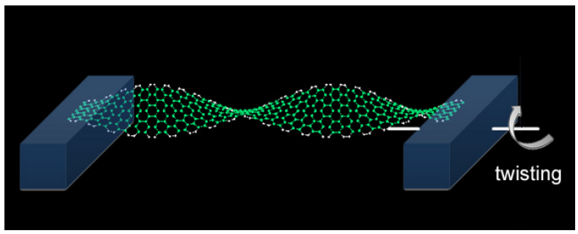

Fig. 1. Schematic illustrations of our model, where an armchair edged GNR (AGNR) is suspended in between two electrodes, and one of the electrodes is allowed to change its angle along the axis threading through AGNR with respect to opposite electrode.

II. Model and Method

A. Model of twisted graphene nanoribbon devices

Figure 1 is the schematic illustration of our model, where an armchair edged GNR (AGNR) is suspended in between two electrodes. We further assume that one of the electrodes is allowed to change its angle along the axis threading through the ribbon with respect to the other electrode.

B. Tight binding molecular dynamics method

In order to obtain the stable structure for a given twisting angle, we employ the structural relaxation based on the tight-binding molecular dynamics (TBMD) method [8], [9], where the electronic energy is calculated quantum mechanically starting from the sp^3 tight binding Hamiltonian, while the repulsive energy due mainly to ion-ion interaction is calculated using the pairwise potential. The TBMD method is advantageous over classical bond order potential method since it allows us to simulate the mechanical and electronics properties of AGNR on the equal footing. Moreover, in order to treat the large number of atoms contained in AGNR within the framework of TBMD, we also employ the order-N algorithm based on the Fermi operator expansion (FOE) method. Below we describe briefly these calculation method. The electronic structure in twisted GNRs can basically be obtained by diagonalizing the standard two-center TB Hamiltonian $H^{ij}_{\alpha\beta}(\boldsymbol{r}_{ij})$, where α (β) is the index of the atomic orbital in the i (j)th atom in the system. Once we calculate the energy eigenvalues (band structure) of the above Hamiltonian, the total energy of the system is given following the TBMD scheme as

$$E_{\rm tot} = E_{\rm bs} + E_{\rm rep}, \tag{1}$$

where $E_{\rm bs}$ is the band structure energy and $E_{\rm rep}$ is the repulsion energy. Here $E_{\rm bs}$ and $E_{\rm rep}$ are respectively calculated as

$$E_{\rm bond} = 2\sum_n \varepsilon_n f\left(\frac{\varepsilon_n - \mu}{k_{\rm B}T}\right), \tag{2}$$

$$E_{\rm rep} = \sum_i f_{\rm poly}\left(\sum_j \phi(r_{ij})\right). \tag{3}$$

In Eq. (2) $f(E)$ is the Fermi distribution function, ε_n the single particle energies obtained from the TB Hamiltonian, and μ the Fermi energy, whereas in Eq. (3) $\phi(r_{ij})$ is a pairwise potential between ith and jth atoms, and $f_{\rm poly}(x)$ is a 4th polynomial function introduced for parameter fittings. Then the total force

ISBN 978-0-615-71756-2

acting on the ith atom is obtained as

$$\boldsymbol{F}_i = -\frac{\partial}{\partial \boldsymbol{R}_i} E_{\rm tot} = -\frac{\partial}{\partial \boldsymbol{R}_i} \left(E_{\rm bs} + E_{\rm rep} \right) = \boldsymbol{F}_i^{\rm bs} + \boldsymbol{F}_i^{\rm rep}, \quad (4)$$

where the 1st term in the RHS can be calculated efficiently as the Hellman-Feynman force

$$\boldsymbol{F}_i^{\rm bs} = \sum_n \left\langle \Psi_n \left| \frac{\partial H}{\partial \boldsymbol{R}_i} \right| \Psi_n \right\rangle f\left(\frac{\varepsilon_n - E_{\rm F}}{k_{\rm B} T} \right), \quad (5)$$

with $|\Psi_n\rangle$ being the nth eigenstate of the TB Hamiltonian. Once the total force acting on the ith atom is obtained, the MD calculation can be performed by solving the Newton's equations

$$M_i \frac{d^2 \boldsymbol{R}_i(t)}{dt^2} = \boldsymbol{F}_i(t), \quad (6)$$

for each ith atom with the mass M_i by applying the standard velocity Verlet method, in which we employed the velocity scaling algorithm to control the kinetic temperature of the system. Then the structural relaxation can be performed by lowering the kinetic temperature gradually to zero until the total energy $E_{\rm tot}$ is converged.

C. Fermi operator expansion method

In the conventional TBMD method, the energy eigenvalue ε_n is calculated by diagonalizing the TB Hamiltonian. Therefore the required computational time for TBMD simulation is basically proportional to $N_{\rm atom}^3$ with $N_{\rm atom}$ being the number of atom contained in the system. In our study, to treat the large number of atoms contained in AGNR within the framework of TBMD, we employ the order-N algorithm based on the Fermi operator expansion (FOE) method [10], [11]. In FOE method, the bandstructure energy $E_{\rm bs}$ is directly calculated by using the Fermi operator F as

$$E_{\rm bs} = 2{\rm Tr}\left[H F_{\mu,T} \right] = 2 \sum_{i\alpha} \langle \varphi_{i\alpha} | H F_{\mu,T} | \varphi_{i\alpha} \rangle, \quad (7)$$

where $|\varphi_{i\alpha}\rangle$ is the atomi orbital. Here the Fermi operator $F_{\mu,T}$ is formally introduced as a matrix representation of the Fermi distribution function as

$$F_{\mu,T} = f\left[\frac{H-\mu}{kT} \right], \quad (8)$$

where the energy argument E in the Fermi distribution function has been formally replaced by the Hamiltonian operator H. Fermi operator becomes a diagonal matrix when it is represented by the energy eigenvector basis set as

$$\langle \Psi_n | F_{\mu,T} | \Psi_m \rangle = f\left[\frac{\varepsilon_n - \mu}{kT} \right] \delta_{n,m}, \quad (9)$$

where ϵ_n is the nth eigenvalue of the Hamiltonian H, and Ψ_n is the corresponding eigenvector. In the actual calculations, the matrix repesentation of the Fermi distribution function is obtaind via the Chebyshev polynomial expansion as

$$F_{\mu,T} = p_{\mu,T}(H), \quad (10)$$

where

$$p_{\mu,T}(H) \equiv \frac{c_0}{2} I + \sum_{l=1}^{N_{\rm pl}} c_l T_l(H). \quad (11)$$

Here $N_{\rm pl}$ is the order of polynomial, and is roughly chosen as

$$N_{\rm pl} \simeq \frac{\varepsilon_{\rm max} - \varepsilon_{\rm min}}{kT}, \quad (12)$$

with $\varepsilon_{\rm max(min)}$ the maximum (minimum) energy eigenvalue in the system, and c_l is the Chebyshev expansion coefficient. Chebyshev matrix polynomial $T_l(H)$ satisfies the following recurrence relations

$$\begin{aligned} &T_0(H) = I, \\ &T_1(H) = H, \\ &T_{l+1}(H) = 2HT_l(H) - T_{l-1}(H), \end{aligned} \quad (13)$$

where I is the identity matrix. The colomn of the matrix $T_l(H)$ with the atomic orbital indices (i,α) is calculated as

$$\begin{aligned} &|t_{i\alpha}^0\rangle = |\varphi_{i\alpha}\rangle, \\ &|t_{i\alpha}^1\rangle = H|\varphi_{i\alpha}\rangle, \\ &|t_{i\alpha}^{l+1}\rangle = 2H|t_{i\alpha}^l\rangle - |t_{l\alpha}^{l-1}\rangle, \end{aligned} \quad (14)$$

where $|\varphi_{i\alpha}\rangle$ is a unit vector with its $i\alpha$th element equal to one and zero otherwise. In the FOE method, the band structure energy is expressed as

$$E_{\rm bs} = 2\sum_{i\alpha} \langle \varphi_{i\alpha} | HF | \varphi_{i\alpha} \rangle = 2 \sum_{i\alpha} \langle H \varphi_{i\alpha} | f_{i\alpha} \rangle, \quad (15)$$

which can be decomposed into the contributions due to the each ith atom. Once the vector $|t_{i\alpha}^l\rangle$ is obtained, $|f_{i\alpha}\rangle$ is obtained as

$$\begin{aligned} |f_{i\alpha}\rangle &= F|\varphi_{i\alpha}\rangle \simeq p_{\mu,T}(H)|\varphi_{i\alpha}\rangle \\ &= \frac{c_0}{2}|t_{i\alpha}^0\rangle + \sum_{l=1}^{N_{\rm pl}} c_l |t_{i\alpha}^l\rangle. \end{aligned} \quad (16)$$

The bond force acting on the jth atom is also expressed in terms of the localized orbital $|\varphi_{i\alpha}\rangle$ as

$$\begin{aligned} \boldsymbol{F}_j &= -\frac{\partial E_{\rm bs}}{\partial \boldsymbol{R}_j} \\ &= -2\sum_{i\alpha} \frac{\partial}{\partial \boldsymbol{R}_j} \langle \varphi_{i\alpha} | HF | \varphi_{i\alpha} \rangle \\ &= -2\sum_{i\alpha} \langle \varphi_{i\alpha} | [p_{\mu,T}(H) + H p'_{\mu,T}(H)] \frac{\partial H}{\partial \boldsymbol{R}_j} | \varphi_{i\alpha} \rangle. \end{aligned} \quad (17)$$

III. Results and Discussions

Figure 2 shows the total energy $E_{\rm tot}$ (i.e., the sum of the bonding and the repulsion energy) of the suspended finite size AGNRs with various widths N (=7, 9, 11) and the fixed length $M = 22$ as a function the twisting angle, where the width N is the number of carbon atoms along the width direction,

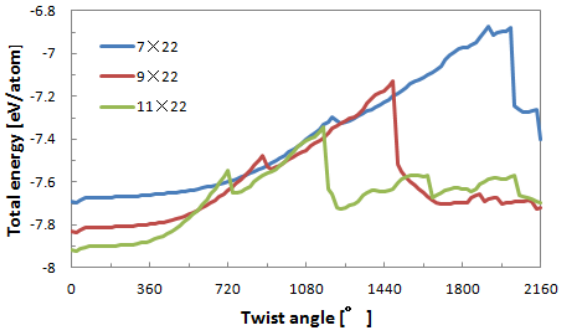

Fig. 2. Twisting angle dependence of the total energy in AGNRs with various widths N.

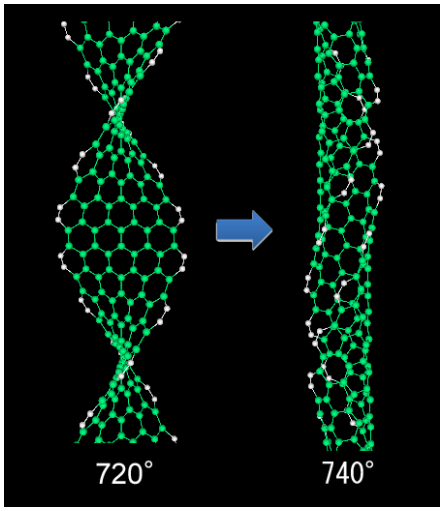

Fig. 3. Abrupt geometrical transition from the ribbon like geometry at 720° to the tube like geometry at 740° for N=11. Here we illustrated the geometrical structure only around the middle section of AGNRs.

while the length M is the number of unit cells along the transport direction. As seen in this figure, the calculated total energy increases first as increasing the twisting angle, but then it shows a small abrupt drop-off at a specific twisting angle that depends on the ribbon N (e.g., at around $\theta = 720°$ for $N = 11$). Such abrupt drop-off of the total energy actually corresponds to the abrupt change in the geometry of the twisted AGNR. That is, an AGNR can be twisted keeping its ribbon like quasi-flat geometry only until a critical twisting angle (Fig. 3, left), over which the ribbon is suddenly rolled up to form tube like geometry (Fig. 3, right), resulting into the sudden decrease of the total energy. Further twisting of the AGNR causes more clear drop-off of the total energy at around $\theta = 1170°$ for $N = 11$, which obviously corresponds to the collapse of the structure. Similar abrupt geometrical transition is seen also for 7×22 ($N = 7$, $M = 22$) AGNR as seen in Fig. 4. Then the next question is how such abrupt change in the geometry of AGNRs influences their electronic

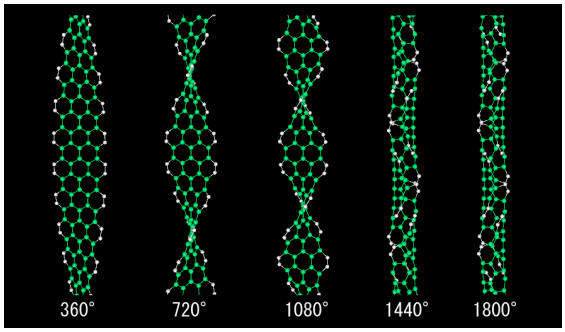

Fig. 4. Relaxed geometrical structures of twisted 7×22 AGNRs with various twisting angles. Here we illustrated the geometrical structure only around the middle section of AGNRs.

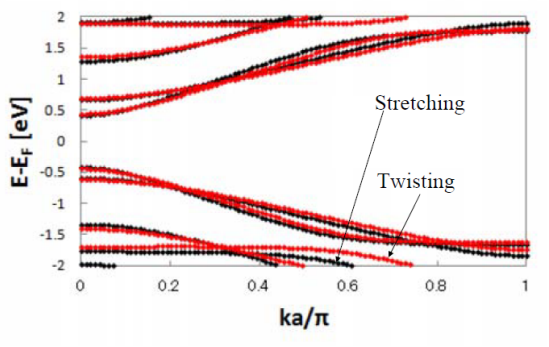

Fig. 5. Band structure of twisted $9\times$ 22 AGNR with the twisting parameter τW=1.55. Here a is the length of the unit cell.

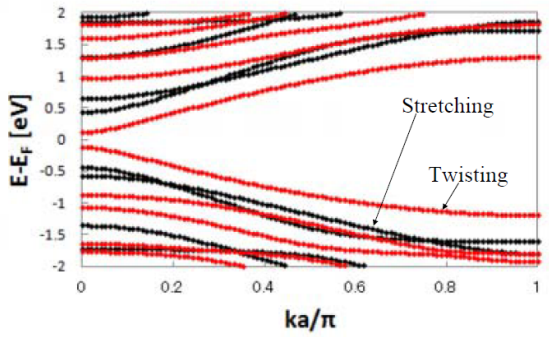

Fig. 6. Band structure of twisted $9\times$ 22 AGNR with the twisting parameter τW=1.62. Here a is the length of the unit cell.

properties.

In order to understand the influence of the abrupt geometrical change seen in Fig. 3, we next consider the band structure estimated from the quasi periodic geometrical structure near the middle region of twisted AGNR. Here we assumed that the twisting induced curvature is enough small so that the Bloch's theorem is approximately valid even in the presence of the twisting, and thus the wavefunctions in two equivalent atoms

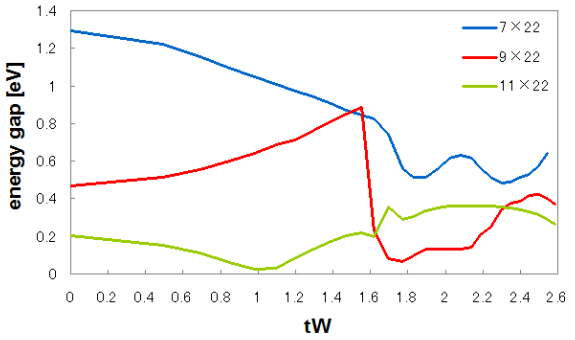

Fig. 7. Calculated band gap observed in the central region of the twisted AGNR as a function of the twisting parameter τW (see the text).

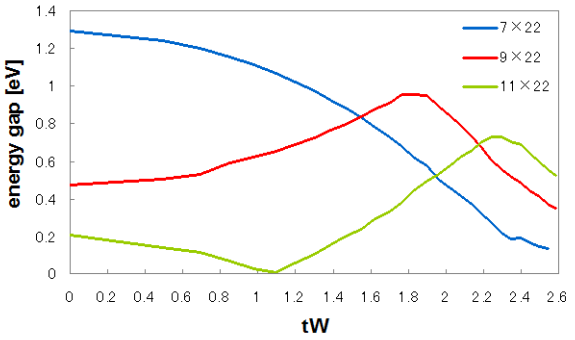

Fig. 8. Calculated band gap observed in the central region of the stretched AGNR as a function of the same parameter τW.

in adjacent unit cells are related by the atom independent phase factor. In Figs. 5 and 6 we plotted the band structures of twisted 9× 22 AGNR with the twisting factor τW=1.55 and 1.65, respectively, where $\tau = \theta/L$ with L being the length of the ribbon, and W the width of the ribbon. For comparison, we also plotted in the each figure the band structures of stretched AGNR, where the stretching ratio SR (defined as SR= $(L' - L)/L$ with L' being the length of AGNR in the stretched case) is adjusted so as to give the same strain energy as for the twisting case for a given value of τW, and is given in terms of the twisting factor τW as [12]

$$\mathrm{SR} = \frac{(\tau W)^2}{24}. \tag{18}$$

We note that these two values of τW used in Figs. 5 and 6 correspond to the twisting angle just before and the after the abrupt geometrical transition seen in Fig. 3. When $\tau W = 1.55$ (before the abrupt geometrical transition), we see in Fig. 5 that the band structure of twisted AGNR is similar to that of stretched AGNR. When τW=1.65 (after the geometrical transition), on the other hand, we see that the band structures of twisted and stretched AGNR are significantly different with each other, meaning that the geometrical transition seen in the twisted AGNR influences the electronic property as well.

Finally in Figs. 7 and 8 we show the band gap observed in the twisted AGNR as a function of the twisting factor τW. By comparing the stretched and twisted cases in Figs. 7 and 8, we can observe that twisted and stretched GNRs show qualitatively the same band gap modulation up to a critical value of τW, over which they started to show rather different behaviors. Obviously, such critical value of τW corresponds to the geometrical transition from the ribbon like geometry to the tube like geometry in the twisted case. Therefore, it is found that the twisting induced abrupt change in the geometry of AGNR can actually cause the abrupt change in the electronic property as well.

IV. Conclusion

We have studied numerically the effect of mechanical twisting on the geometrical and electronic properties of graphene nanoribbon (GNR) devices. By employing the tight-binding molecular dynamics method for structural relaxation calculations in the presence of twisting, we found that the geometry of the twisted GNR changes abruptly when the twisting angle exceeds a threshold angle. Moreover it has been found that such twisting induced abrupt change in the geometry of AGNR can actually causes the abrupt change in the electronic property as well.

References

[1] K. S. Novoselov, A. K. Geim, S. V. Morozov, D. Jiang, Y. Zhang, S. V. Dubonos, I. Grigorieva, and A. A. Firsov, "Electric Field Effect in Atomically Thin Carbon Films", Science. **306**, 666 (2004).

[2] K. S. Novoselov, A. K. Geim, S. V. Morozov, D. Jiang , M. I. Katsnelson , I. V. Grigorieva , S. V. Dubonos, and A. A. Firsov, "Two-dimensional gas of massless Dirac fermions in graphene", Nature **438**, 197 (2005).

[3] M. I. Katsnelson, K. S. Novoselov, and A. K. Geim, "Chiral tunnelling and the Klein paradox in graphene", Nature **2**, 620 (2006).

[4] M. Fujita, K. Wakabayashi, K. Nakada, and K. Kusakabe, "Peculiar Localized State at Zigzag Graphite Edge", J. Phys. Soc. Jpn. **65**, 1920 (1996).

[5] Y-W Son, M. L. Cohen, and S. G. Louie, "Half-metallic graphene nanoribbons", Nature **444**, 347 (2006) .

[6] C. Tao, L. Jiao, O. V. Yazyev, Y.-C. Chen, J. Feng, X. Zhang, R. B. Capaz, J. M. Tour, A. Zettl, S. G. Louie, H. Dai, and M. F. Crommie, "Spatially resolving edge states of chiral graphene nanoribbons", Nature Phys. **7**, 616 (2011).

[7] S. Souma, M. Ogawa, T. Yamamoto, K. Watanabe, "Numerical Simulation of Electronic Transport in Zigzag-edegd Graphene Nano-Ribbon Devices", J. Comput. Electron. **7** 390 (2008).

[8] L. Goodwin, A. J. Skinnner, D. G. Pettifor, "Generating Transferable Tight-Binding Parameters: Application to Silicon", Europhys. Lett., **9**, 701 (1989).

[9] C. H. Xu, et al, "A transferable tight-binding potential for carbon," J. Phys. Condens. Matter **4**, 6047 (1992).

[10] S. Goedecker, L. Colombo, "Efficient Linear Scaling Algorithm for Tight-Binding Molecular Dynamics," Phys. Rev. Lett., **73** 122 (1994).

[11] S. Goedcker and M. Teter, "Tight-binding electronic-structure calculations and tight-binding molecular dynamics with localized orbitals," Phys. Rev. B **51**, 9455 (1995).

[12] Y. Li, "Twist-enhanced stretchability of graphene nanoribbons: a molecular dynamics study," J. Phys. D **43**, 495405 (2010).